Synthesis and Characterization of Thermally Responsive Pluronic F127—Chitosan Nanocapsules for Controlled Release and Intracellular Delivery of Small Molecules

Wujie Zhang,[†,‡] Kyle Gilstrap,[†,‡] Laying Wu,[§] Remant Bahadur K. C.,[†,‡] Melissa A. Moss,[‡,⊥,¶] Qian Wang,[§,¶] Xiongbin Lu,[∥] and Xiaoming He[†,‡,¶,*]

[†]Department of Mechanical Engineering, [‡]Biomedical Engineering Program, [§]Department of Chemistry and Biochemistry, [⊥]Department of Chemical Engineering, [∥]Department of Biological Sciences, and [¶]NanoCenter, University of South Carolina, Columbia, South Carolina 29208, United States

ABSTRACT In this study, we synthesized empty core—shell structured nanocapsules of Pluronic F127 and chitosan and characterized the thermal responsiveness of the nanocapsules in size and wall-permeability. Moreover, we determined the feasibility of using the nanocapsules to encapsulate small molecules for temperature-controlled release and intracellular delivery. The nanocapsules are ~37 nm at 37 °C and expand to ~240 nm when cooled to 4 °C in aqueous solutions, exhibiting >200 times change in volume. Moreover, the permeability of the nanocapsule wall is high at 4 °C (when the nanocapsules are swollen), allowing free diffusion of small molecules (ethidium bromide, MW = 394.3 Da) across the wall, while at 37 °C (when the nanocapsules are swollen), the wall-permeability is so low that the small molecules can be effectively withheld in the nanocapsule for hours. As a result of their thermal responsiveness in size and wall-permeability, the nanocapsules are capable of encapsulating the small molecules for temperature-controlled release and intracellular delivery into the cytosol of both cancerous (MCF-7) and noncancerous (C3H10T1/2) mammalian cells. The cancerous cells were found to take up the nanocapsules much faster than the noncancerous cells during 45 min incubation at 37 °C. Moreover, toxicity of the nanocapsules as a delivery vehicle was found to be negligible. The Pluronic F127—chitosan nanocapsules should be very useful for encapsulating small therapeutic agents to treat diseases particularly when it is combined with cryotherapy where the process of cooling and heating between 37 °C and hypothermic temperatures is naturally done.

KEYWORDS: nanocapsule · thermal responsiveness · Pluronic F127 · chitosan · controlled release · intracellular delivery · wall-permeability

Nanoscale particulate systems have been studied as the delivery vehicle of various drugs and therapeutic agents for decades with promising outcomes.[1−5] Recently, nanoparticulate systems that are responsive to one or more environmental stimuli (such as temperature, pH, and electromagnetic field) are attracting more and more attention because they allow drug delivery and release to be done in a more controllable fashion.[6−12] The thermally (temperature) responsive nanoparticles are of particular interest to many researchers because the temperature-controlled release of the encapsulated drug can be conveniently done with either thermo (using supraphysiologic temperatures) or cryo (using subzero temperature) therapies, minimally invasive energy-based surgical techniques that have been widely studied as potential alternatives to the radical surgical intervention for the treatment of cancer and various other diseases. Moreover, a significantly improved outcome of cancer treatment has been reported by combining thermotherapy (using supraphysiologic temperatures) and anticancer drug encapsulated in thermally responsive nanoparticles (liposomes).[13−19]

Besides liposomes, thermally responsive nanoparticles have also been made using various polymers including Pluronics.[20−34] Pluronics are amphiphilic, triblock copolymers composed of poly(oxyethylene)-block-poly(oxypropylene)-block-poly(oxyethylene) (PEO_x-PPO_y-PEO_z) that are commonly used as nonionic macromolecular surfactants with excellent biocompatibility.[34−37] Due to their amphiphilic nature, Pluronic copolymers form micelles (either solid or with an empty core) in an oil-in-water emulsion with the more hydrophobic PPO and hydrophilic PEO blocks being oriented to the oil and water phases, respectively. These micellar structures can be made permanent to produce thermally responsive nanocapsules by cross-linking the Pluronic polymer with cross-linkers such as heparin and polyethylenimine (PEI).[28−33] For example, the

*Address correspondence to xmhe@sc.edu.

Received for review July 12, 2010 and accepted October 25, 2010.

Published online November 1, 2010. 10.1021/nn101617n

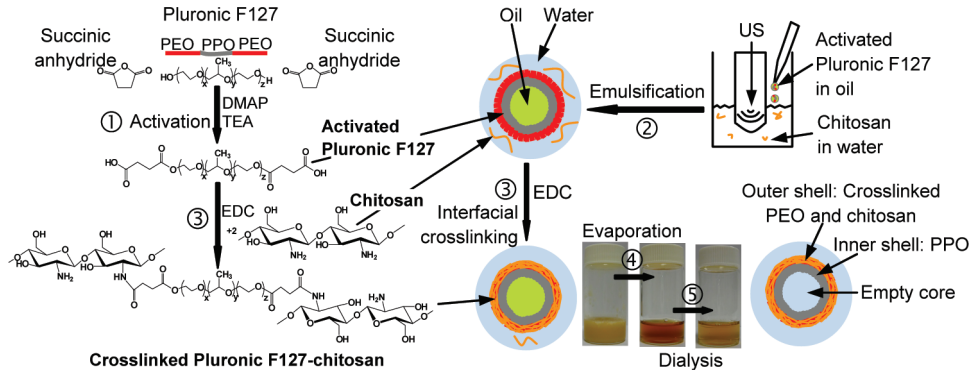

Figure 1. Illustration of the chemistry and procedures to synthesize the Pluronic F127−chitosan nanocapsules. The pictures show the typical appearance of the oil-in-water emulsion before rotary evaporation, after rotary evaporation to remove the organic oil phase, and after dialysis to remove the catalyst (EDC) and any residual polymers. The oil used is dichloromethane. PPO, polypropylene oxide; PEO, polyethylene oxide; DMAP, 4-dimethylaminopyridine; TEA, triethylamine; EDC, 1-ethyl-3-[3-dimethylaminopropyl]carbodiimide hydrochloride; US, ultrasound.

Pluronic F127 (PEO_{100}-PPO_{65}-PEO_{100})-based nanocapsules made in this way have been reported to exhibit a volume change of more than 1000 and 20−40 times between 4 and 37 °C in aqueous solutions when heparin and PEI are used as the cross-linker, respectively.[30−33] Beside their thermal responsiveness in size, our recent studies demonstrate that the wall-permeability of the Pluronic F127−PEI nanocapsules is thermally responsive, as well.[33] Moreover, we have successfully utilized the thermal responsiveness of the Pluronic F127−PEI nanocapsules in size and wall-permeability to encapsulate a small molecule (trehalose, MW = 342 Da) for delivery into the cytosol of mammalian cells.[33] However, the potential cytotoxicity of PEI is a concern particularly for translational and clinical applications.[38−41]

In this study, we report the synthesis and characterization of the Pluronic F127-based nanocapsules using chitosan as the cross-linker. The Pluronic F127−chitosan nanocapsules were found to have excellent biocompatibility, presumably due to the biocompatible nature of the two constituent polymers: Pluronic F127 has been approved by FDA (Food and Drug Administration) for use as food additives and pharmaceutical ingredients,[34−37] and chitosan is a natural, cationic polysaccharide that is commonly found in seafood.[42−47] Moreover, we found that the Pluronic F127−chitosan nanocapsules can be used to encapsulate small molecules (ethidium bromide, MW = 394.3 Da) for intracellular delivery (by incubating with mammalian cells at 37 °C for 45 min in serum-free medium) and temperature-controlled release in the cells.

RESULTS

Surface Chemistry, Morphology, and Size of the Pluronic F127−Chitosan Nanocapsules. The chemistry of the Pluronic activation and nanocapsule synthesis is shown in Figure 1. Pluronic F127 was activated by adding a carboxyl group (−COOH) to both ends of the polymer. The activation efficiency was determined to be 91.8 ± 2.3% using the acid−base titration method. During the nanocapsule synthesis, EDC was used to catalyze the reaction (formation of cross-link) between the carboxyl group of activated Pluronic F127 and the amine group of chitosan to form amide bonds.[48,49] Successful preparation of the thermally responsive Pluronic F127−chitosan was confirmed by ^{1}H NMR, FTIR, TEM, and DLS analysis.

The ^{1}H NMR and FTIR spectra of the activated Pluronic F127 and chitosan cross-linked Pluronic F127 (feeding at 10% for synthesis) nanocapsules are shown in Figure 2A,B, respectively. The ^{1}H NMR spectrum of the activated Pluronic F127 shows a prominent resonance peak at δ ∼2.55 ppm corresponding to the methylene protons (−C$\underline{H_2}$−C$\underline{H_2}$−) of the succinic groups added to the terminals of Pluronic F127 along with the major resonance peaks of Pluronic F127 (at δ ∼1.05 and 3.2−3.8 ppm). The ^{1}H NMR spectrum of the chitosan cross-linked Pluronic F127 nanocapsules shows the major peaks of activated Pluronic F127 along with the resonance peaks at δ ∼1.9 and 2.7 ppm corresponding to the methyl (−C$\underline{H_3}$) and methylene proton at the C2 position of chitosan, respectively.[50] The cross-linking between chitosan and the activated Pluronic F127 through an amide bond at the terminal end of the polymers was confirmed by the splitting of the methylene resonance peaks (δ ∼2.55 ppm) into two at δ ∼2.55 and 2.35 ppm. These changes in chemical shift of the protons in the $-CH_2-CH_2-COOH$ group are typical when the terminal carboxyl group is reacted with the amine group to form amide bonds (Figure 1). By integrating the proton resonance peaks of chitosan (at δ ∼2.55 ppm) and Pluronic F127 (at δ ∼1.05 ppm), chitosan was found to take up ∼11% (by weight) of the nanocapsules.

When comparing the FTIR spectrum of Pluronic F127 before and after activation (Figure 2B), a peak at 1735 cm^{-1} as a result of C═O stretching in the carboxyl (−COOH) group is noticeable only for the activated polymer, indicating the −COOH group was success-

fully added to the two terminals of Pluronic F127 after activation. The FTIR spectrum of chitosan shows two peaks at 1637 and 1560 cm^{-1} as a result of the strong N−H bending (1560 cm^{-1}) in the primary amine ($-NH_2$) groups and the amide I (C═O stretching, 1637 cm^{-1}) and amide II (weaker N−H bending than that in the primary amine, 1560 cm^{-1}) in the residual (5%) acetylated amine ($-NH-(C{=}O)-CH_3$) groups of chitosan.[49,51] In the spectrum of Pluronic F127−chitosan nanocapsules, however, the amides II peak at 1560 cm^{-1} is barely identifiable while the amide I peak at 1637 cm^{-1} is apparent. The diminished amide II peak presumably is due to the loss of primary amine ($-NH_2$) groups to the secondary (−NH−) ones when chitosan is cross-linked with the activated Pluronic F127, which at the same time strengthens the amide I peak as a result of the formation of more amide bonds.[52,53] Moreover, the peak of C═O stretching (1735 cm^{-1}) in the carboxyl group is significantly weakened in the spectrum of the nanocapsule compared with that in the activated Pluronic F127, presumably due to formation of the amide bond between the carboxyl group in the activated Pluronic F127 and the primary amine groups in chitosan. The presence of the C═O stretching peak at 1735 cm^{-1} in the FTIR spectrum of the nanocapsules indicates that not all of the activated terminals of Pluronic F127 in the nanocapsules formed an amide bond with chitosan. In summary, all of these observations indicate the conjugation of chitosan onto Pluronic F127 *via* the formation of amide bonds between the two polymers during the nanocapsule synthesis process.

To investigate the effect of EDC catalysis time on the nanocapsule synthesis, Pluronic F127(10%)−chitosan nanocapsules were prepared by allowing various durations (0−20 h) of EDC catalysis. FTIR spectra of the various nanocapsules formed are shown in Figure 3A. We further quantified the area ratio of peak 1 (for amide I) to peak 2 (for glucosamine, the building unit of chitosan to serve as the reference of the amount of chitosan present in the nanocapsules), and the results are shown in Figure 3B. The relative peak area significantly increases with the increase of the EDC catalysis time in ~10 h and reaches a plateau thereafter, which indicates that more amide bonds formed (or more chitosan cross-linked onto Pluronic F127) with the increase of catalysis time in the first 10 h during the synthesis process.

We further studied the effect of the EDC catalysis time on the nanocapsule synthesis and morphology using TEM, and the results are shown in Figure 4. Morphologically, an empty core−shell structure was clearly visible for all of the nanocapsules synthesized in the absence of EDC (0 h catalysis, Figure 4A). By allowing a short EDC catalysis (10 min, with 4 min for emulsification and 6 min for rotary evaporation, steps 1−4 in Figure 1) of the cross-linking reaction between the activated Pluronic F127 and chitosan during the synthesis process, the empty core−shell structure became invisible in some of the nanocapsules (Figure 4B). Moreover, after 20 h catalysis, the empty core−shell structure is not observable in any of the nanocapsules, which also appear much denser (darker) than the nanocapsules with observable empty core−shell structure (Figure 4C). The morphological difference observed may be explained by the difference of chitosan contents and the extent of cross-link formation between the activated Pluronic F127 and chitosan in the nanocapsules formed with various times of EDC catalysis. For the nanocapsule prepared without EDC catalysis, chitosan and the activated Pluronic F127 probably are attached to each other to form a loose mixture as a result of their opposite electric charges (positive for chitosan and negative for the activated Pluronic F127) without forming any amide bond because the cross-link reaction is extremely slow in the absence of EDC catalysis. As a result of the loose structure in the wall of the nanocapsule (or more exactly, nanocomplex), the empty core−shell structure

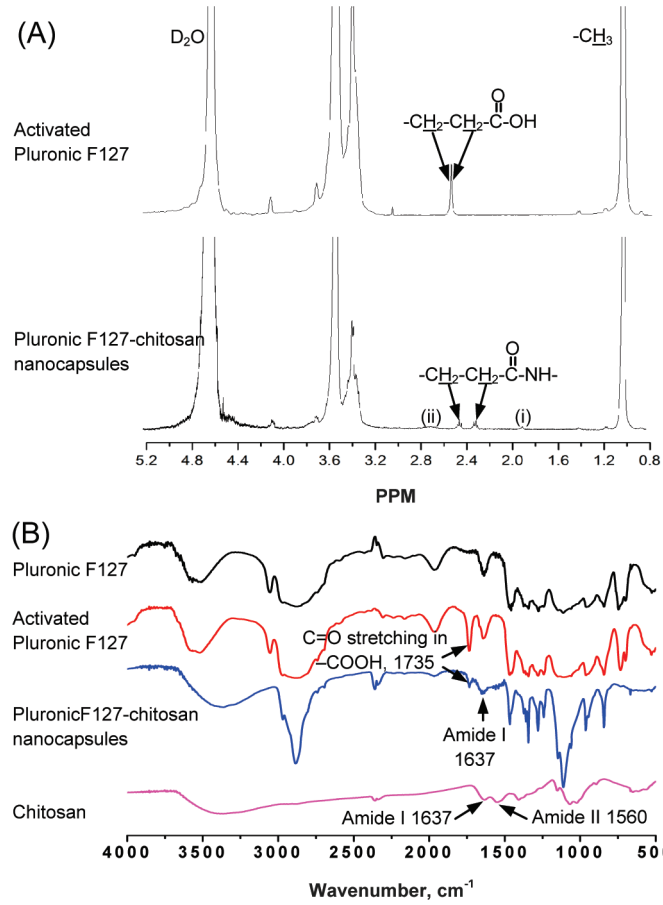

Figure 2. Typical ^1H NMR spectra (A) of activated Pluronic F127 and the Pluronic F127(10%)−chitosan nanocapsules (20 h cross-linking) and FTIR spectra (B) of the Pluronic F127(10%)−chitosan nanocapsules, chitosan, Pluronic F127, and activated Pluronic F127 showing successful activation of Pluronic F127 and cross-link formation between the activated Pluronic F127 and chitosan in the Pluronic F127−chitosan nanocapsules: (i) and (ii) indicate the resonance peaks at δ ~1.9 and 2.7 ppm corresponding to the methyl ($-CH_3$) and methylene proton at the C2 position of chitosan, respectively.

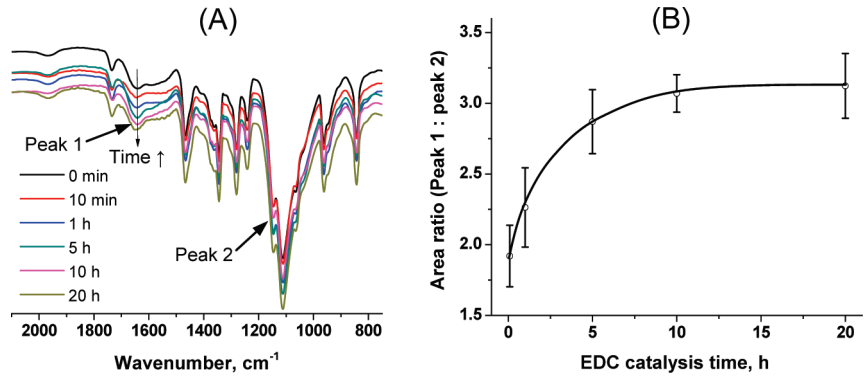

Figure 3. FTIR spectra of the Pluronic F127(10%)−chitosan nanocapsules prepared by allowing different times for cross-linking (A) and the area ratio of peak 1 (amide I) to peak 2 (glucosamine, the building unit of chitosan) illustrating the change in the extent of cross-link formation in the nanocapsules with the EDC catalysis time (B). The error bars represent the standard deviation.

is evident. With the formation of more amide bond and addition of more chitosan, the wall of the nanocapsule should become denser and tighter as the EDC catalysis time increased, which ultimately made the empty core−shell structure invisible in the TEM image even though the lumen was still there. Interestingly, the nanocapsule without a visible empty core−shell structure also appears smaller than those with a visible empty core−shell structure, probably because the polymers in the nanocapsule wall became more tightened with the formation of the covalent amide bond of the cross-link.

The size of the nanocapsules in 1× PBS was further studied quantitatively by dynamic light scattering (DLS) at various temperatures from 4 to 45 °C, and the results are shown in Figure 5. A broad thermal responsiveness over the temperature range is observable for the nanocapsules. A schematic illustration of the nanocapsule at 4 and 37 °C is also shown in the figure. Overall, the nanocapsules exhibit a change in diameter (D) and volume ($V \propto D^3$) of more than 6 and 200 times between the two temperatures, respectively. Moreover, the thermally responsive properties are dependent on the EDC catalysis time and the feeding percentage of the activated Pluronic F127 during synthesis. For example, the Pluronic F127(10%)−chitosan nanocapsules synthesized with 10 min EDC catalysis are bigger than that synthesized with 20 h EDC catalysis at or below room temperature, which is consistent with the TEM data shown in Figure 4. Moreover, by allowing 20 h EDC catalysis, the use of more activated Pluronic F127 (30 *vs* 10%) to synthesize the nanocapsule significantly affects the temperature range (~25−30 *vs* 15−37 °C) over which the thermal responsiveness occurs, although the nanocapsule size either below 15 °C or above 37 °C is not significantly affected. Interestingly, the temperature range over which the thermal responsiveness occurs for the nanocapsule synthesized with 10% activated Pluronic F127 and 10 min EDC catalysis is closer to that for the nanocapsule synthesized with 30% Pluronic and 20 h EDC catalysis than that for the nanocapsules synthesized with 10% Pluronic and 20 h EDC catalysis. These observations suggest that the temperature range over which the thermal responsiveness occurs narrows with the increase of Pluronic F127 with regard to the amount of chitosan (or the extent of cross-link formation) in the nanocapsule wall. Moreover, the cross-link in the nanocapsule wall could stop the expansion of the nanocapsules at low temperatures (*e.g.*, <15 °C) but appears to have minimal impact on the nanocapsule contraction at high temperatures (*e.g.*, >37 °C).

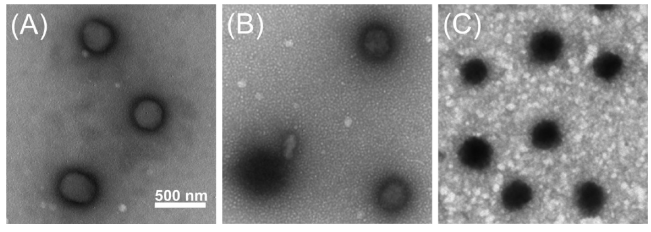

Figure 4. Typical TEM images of Pluronic F127(10%)−chitosan nanocapsules prepared by allowing no EDC catalysis (A), 10 min EDC catalysis (B), 20 h EDC catalysis (C) of the cross-link formation. The scale bar shown in panel A also applies to panels B and C.

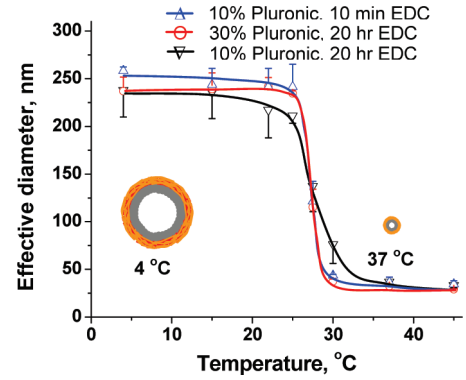

Figure 5. DLS (dynamic light scattering) data of the effective diameter of Pluronic F127−chitosan nanocapsules prepared under three different conditions as indicated in the figure legend. Also shown in the figure is a schematic illustration of the thermal responsiveness of the nanocapsules in size between 4 and 37 °C. The error bars represent the standard deviation.

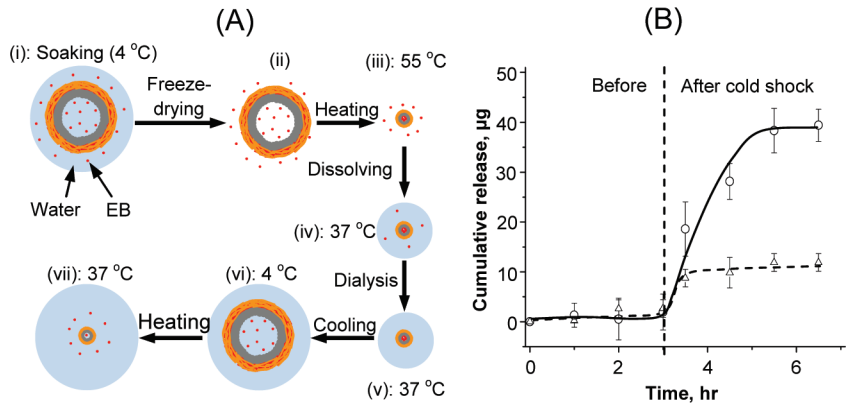

Figure 6. (A) Schematic illustration of the procedure for encapsulating (i−v) ethidium bromide (EB) in the Pluronic F127−chitosan nanocapsules and the cold shock treatment (v−vii) to achieve temperature-controlled release of the encapsulated EB and (B) cumulative release of EB encapsulated in the Pluronic F127−chitosan nanocapsules synthesized using either 30% (circle) or 10% (triangle) Pluronic F127 out of the nanocapsules into water in the 1 mL dialysis tube and further into the 45 mL deionized water outside the dialysis tube at 37 °C before and after the cold shock treatment at 3 h. The error bars represent the standard deviation.

Encapsulation of Ethidium Bromide (EB) for Controlled Release and Intracellular Delivery. A schematic illustration of the procedure for encapsulating EB in the Pluronic F127−chitosan nanocapsules is given as steps i−v in Figure 6A. Briefly, EB was loaded into the nanocapsules (20 h cross-link formation during synthesis) by soaking (i) the probe (3 mg) and nanocapsules (10 mg) in water (300 μL) at 4 °C when the nanocapsules are swollen with a high wall-permeability. After soaking, the sample was freeze-dried (i,ii) to remove water altogether. The dried mixture of free and encapsulated EB was then heated (ii,iii) to shrink the nanocapsules. The sample was then dissolved (iii,iv) in 37 °C DI water and dialyzed (iv,v) against DI water to remove any free (non-encapsulated) EB. The amount of EB encapsulated in the 10 mg nanocapsules was determined colorimetrically to be 41.8 ± 1.7 and 13.7 ± 1.6 μg for the nanocapsules synthesized using 30 and 10% Pluronic F127, respectively. In other words, the encapsulation capacity (or payload) is 4.18 ± 0.17 and 1.37 ± 1.6 μg(EB)/mg(nanocapsules) for the two nanocapsules under the above loading/encapsulation conditions. The much lower encapsulation capability of the Pluronic F127(10%)−chitosan nanocapsules compared to that of the Pluronic F127(30%)−chitosan nanocapsules suggests that the wall-permeability of the former probably is not as low as that of the latter at 37 °C to hold the small molecules. Consequently, a significant amount of EB might leak out of the Pluronic F127(10%)−chitosan nanocapsules during the rigorous washing (iv, v in Figure 6A) at 37 °C to remove free EB, resulting in the much reduced encapsulation payload under the same loading conditions. Of note, the encapsulation capacity is also dependent on the properties (molecular weight/size, solubility, and chemical structure) of the probe used.

Release of the encapsulated EB out of the nanocapsules into the dialysis tube (1 mL) and further into the 45 mL DI water outside the dialysis tube at 37 °C is shown in Figure 6B. When kept at 37 °C for 3 h, the amount of EB in the 45 mL dialysate was negligible. Moreover, after a cold shock treatment (steps v−vii in Figure 6A) of the 1 mL sample in the dialysis tube to liberate the EB from the nanocapsules, a burst release of the probe into the 45 mL DI water was evident. The release reached equilibrium in approximately 2.5 and 0.5 h after the cold shock treatment for the nanocapsules synthesized using 30 and 10% Pluronic F127, respectively. Of note, the 0.5 and 2.5 h times are for the probe to diffuse through the wall of dialysis tube into the 45 mL dialysate. Apparently, it takes more time for the diffusion to reach equilibrium if there are more probes in the dialysis tube. Release of the probe from the nanocapsules into the 1 mL water in dialysis tube should be instant.[33] The total amount of EB released into the 45 mL dialysate was determined to be 39.4 ± 3.2 and 11.9 ± 1.8 μg for the two nanocapsules, which is approximately 94 and 87% of the total amount of EB encapsulated in 10 mg of the two nanocapsules. This slight difference in the release percentage of EB per cold shock treatment probably is due to experimental variations and the slight difference in thermal responsiveness of the two nanocapsules between 4 and 37 °C, as shown in Figure 5 (20 h EDC catalysis): the nanocapsules synthesized using 10% Pluronic F127 are slightly bigger at 37 °C than that synthesized using 30% Pluronic F127, although their sizes are quite similar at 4 °C on average. These results indicate that the wall-permeability of the Pluronic F127−chitosan nanocapsules is indeed thermally responsive and can be used to encapsulate small molecules for controlled release using a procedure shown in Figure 6A. Moreover, the concentration of the Pluronic F127 (and presumably the concentration of chitosan and the time for EDC catalysis) used for synthesizing the nanocapsules can significantly affect the wall-permeability and thus the capability of the nanocapsules for encapsulating small molecules.

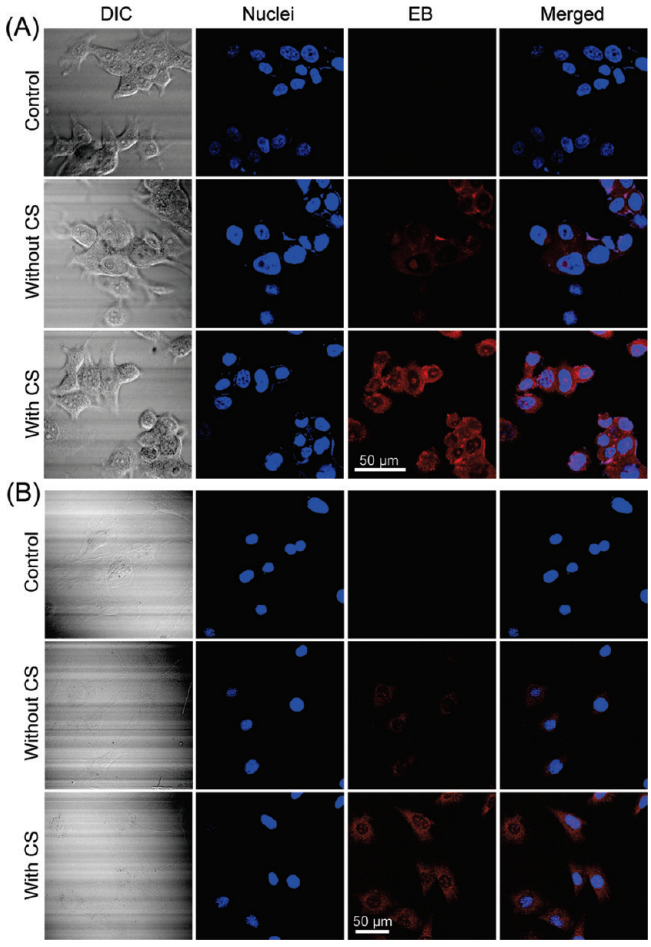

Figure 7. Typical confocal micrographs showing the morphology (DIC, differential interference contrast), nuclei (stained blue using Hoechst 33342), intracellular EB (red), and the merged view of the blue and red channels of the MCF-7 (A) and C3H10T1/2 (B) cells after incubated (at 37 °C for 45 min) in serum-free culture medium containing 0.5 mg/mL Pluronic F127(30%)−chitosan nanocapsule loaded with EB either with or without a cold shock (CS) treatment at 4 °C. The control cells were incubated in serum-free culture medium without any EB-loaded nanocapsules. The scale bar in each panel applies to all micrographs in the same panel.

We further investigated the capability of the Pluronic F127(30%)−chitosan nanocapsules in carrying the encapsulated EB for temperature-controlled release inside living cells. Typical confocal images showing such capability of the nanocapsules are given in Figure 7A,B for MCF-7 and C3H10T1/2 cells, respectively. The DIC (differential interference contrast) images show the cell morphology, which is clear for the MCF-7 cells but not as clear for the C3H10T1/2 cells probably because they spread much thinner than the MCF-7 cells. The cell nuclei were stained blue using Hoechst 33342 and are clearly visible for both cells. Successful intracellular delivery of EB (red fluorescence) is evident for MCF-7 cells incubated with the EB-loaded nanocapsules either without or with a cold shock treatment but not in the control cells that are incubated in serum-free medium without any EB-loaded nanocapsules. For the C3H10T1/2 cells, the red fluorescence is evident in the cells with a cold shock treatment (although it is not as clearly visible in the cells without cold shock), indicating successful delivery of EB into the cells, as well. The red fluorescence in the C3H10T1/2 cells is constantly weaker than that in the MCF-7 cells, indicating the cell-type-dependent uptake of the EB-loaded Pluronic F127−chitosan nanocapsules: the cancerous MCF-7 cells could take up the nanocapsules much faster than the noncancerous C3H10T1/2 cells, which presumably can be attributed to the much faster metabolic and endocytotic activity in cancerous cells. Moreover, the intracellular red fluorescence is much stronger after cold shock in both cells. Presumably, this observation is a result of the temperature-controlled release of EB from the nanocapsules into the cytosol of the cells with cold shock, as shown in Figure 6A (v−vii). This is because the free EB in the cytosol tends to intercalate with both RNAs and DNA (without appreciable base pair specificity) in cells, leading to more than 10 times increase in fluorescence intensity.[54−59] These results indicate the feasibility of using the Pluronic F127−chitosan nanocapsules to encapsulate small molecules for not only delivery into both cancerous and noncancerous cells but also temperature-controlled release of the molecules in the cells.

Cellular Uptake of the Pluronic F127−Chitosan Nanocapsules Labeled with Fluorescence Probe (FITC). To further our understanding of cellular uptake of the Pluronic F127−chitosan nanocapsules, we labeled the nanocapsules (synthesized using 10% Pluronic F127) with FITC (a green fluorescence probe) permanently and stained the endosome/lysosome system in MCF-7 cells using LysoTracker Red (a red fluorescence probe). Typical confocal micrographs showing cellular uptake of the FITC-labeled nanocapsules, and their intracellular distribution is given in Figure 8 for MCF-7 cells either without (top panels) or with (bottom panels) a cold shock treatment at 4 °C for 15 min. The cell morphology is shown in the DIC images, and the cell nuclei were stained blue using Hoechst 33342. Cellular uptake of the FITC-labeled nanocapsules is demonstrated by the apparent green fluorescence in cells either without or with the cold shock treatment. Moreover, many more spotted locations with bright green fluorescence are visible in the cells without cold shock, while the green fluorescence in cells with cold shock is much more homogeneous. Interestingly, many more spotted locations with bright red fluorescence representing endosome/lysosome are also visible in cells without cold shock. Furthermore, the spotted locations with bright red and green fluorescence overlap in the cells without cold shock, resulting in the spotted, bright, yellowish appearance in the merged view of the green and red channels. These observations indicate that endocytosis *via* the endosome/lysosome system is an important mechanism for cellular uptake of the Pluronic F127−chitosan nanocapsules. The bright, yellowish spot is not readily identifiable in the merged view for

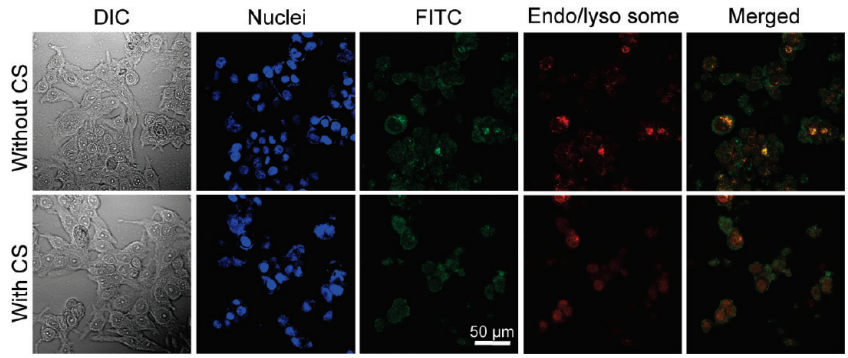

Figure 8. Typical confocal micrographs showing the morphology (DIC), nuclei (stained blue using Hoechst 33342), intracellular nanocapsules (labeled green using FITC), endosome/lysosome (stained red using LysoTracker Red), and the merged view of the green and red channels of MCF-7 cells after incubated (at 37 °C for 45 min) with the FITC-labeled Pluronic F127(10%)−chitosan nanocapsules (0.5 mg/mL) in serum-free culture medium containing 50 nM LysoTracker Red either with or without cold shock (CS) at 4 °C for 15 min. The control cells were incubated in serum-free medium without any nanocapsules. The scale bar applies to all micrographs in the figure.

cells with cold shock, which presumably is due to breaking the endosome/lysosome by the nanocapsules as a result of the significant (more than 200 times) volume expansion of the nanocapsules in response to cooling during cold shock. As shown in Figure 5, the diameter (~240 nm) of the nanocapsules at 4 °C is much bigger than that of the endosome/lysosome (~150 nm).[60,61]

Cytotoxicity of Pluronic F127−Chitosan Nanocapsules. The immediate cell viability and 3 day proliferation of both MCF-7 (Figure 9A,C) and C3H10T1/2 (Figure 9B,D) cells after being exposed to the Pluronic F127(30%)−chitosan nanocapsules (45 min at 37 °C followed by a cold shock at 4 °C for 15 min) at different extracellular concentrations from 0 to 10 mg/mL are shown in Figure 9. The immediate cell viability was more than 99% on average under all of the experimental conditions for both cells. Moreover, the 3 day proliferation of the cells exposed to nanocapsules up to 10 mg/mL was not significantly different from that of control (0 mg/mL) for both the MCF-7 (Figure 9C) and C3H10T1/2 (Figure 9D) cells. Since a significant amount of nanocapsules could be taken up by the cells during the 45 min incubation period and the nanocapsules could escape the endosome/lysosome system in response to a cold shock treatment as demonstrated in Figures 7 and 8, the results shown in Figure 9 (*i.e.*, high immediate cell viability and normal proliferation in 3 days) indicate that toxicity of the Pluronic

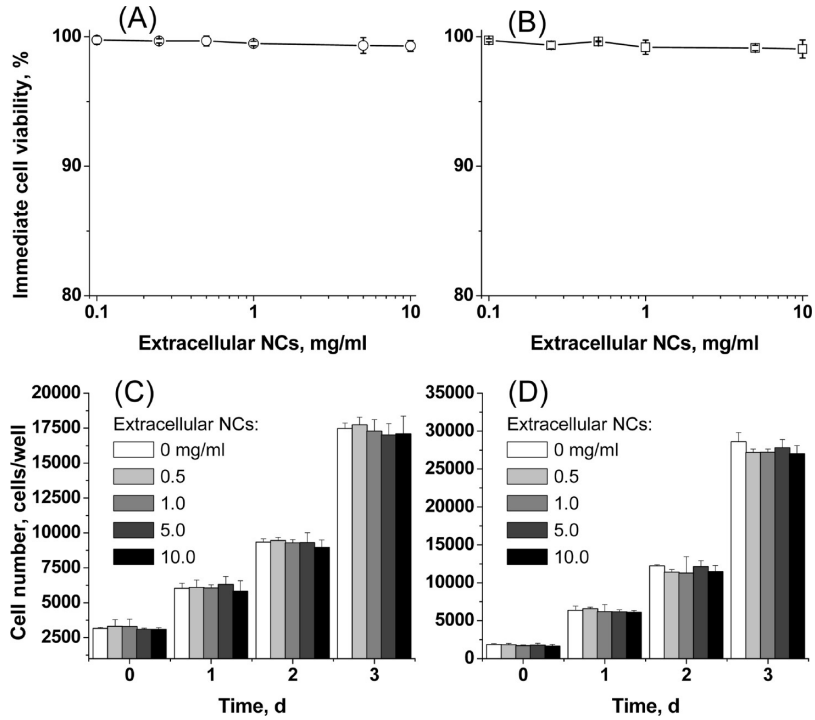

Figure 9. Immediate cell viability and 3 day proliferation of MCF-7 (A,C) and C3H10T1/2 (B,D) cells after incubated with serum-free medium containing 0−10 mg/mL Pluronic F127(30%)−chitosan nanocapsules (NCs) at 37 °C for 45 min followed by cold shock at 4 °C in fresh culture medium. The error bars represent standard deviation.

F127−chitosan nanocapsules to either the cancerous (MCF-7) or noncancerous (C3H10T1/2) cells is negligible, at least for the concentrations tested. Moreover, the process of breaking the endosome/lysosome system by a cold shock treatment to release the nanocapsules into the cytosol did not result in significant injury to the cells either.

DISCUSSION

Pluronic F127 is an amphiphilic triblock copolymer with a formula PEO_{100}-PPO_{65}-PEO_{100}, in which the subscripts 100 and 65 indicate the number of PEO (polyethylene oxide) and PPO (polypropylene oxide) blocks per molecule, respectively. A distinctive feature of Pluronic copolymers is that they exhibit a sol−gel transition behavior in aqueous solution when temperature increases from below to above its lower critical solution temperature (LCST).[61,62] The solution to gel transition is accompanied with a significant volume contraction as a result of dehydration of the PPO blocks (*i.e.*, the PPO blocks become more hydrophobic with the increase of temperature), which is presumably responsible for the significant volume change (*e.g.*, more than 200 times contraction from 4 to 37 °C) observed for the nanocapsules synthesized in this study. Such volume change has also been reported for other Pluronic F127-based nanocapsules. For example, the volume contraction from 4 to 37 °C of Pluronic F127−PEI (polyethylenimine) nanocapsules was found to be 20−40 times,[31−33] and it is more than 1000 times for Pluronic F127−heparin nanocapsules.[30] The volume contraction of the Pluronic F127−chitosan nanocapsules reported in this study is between those of the PEI and heparin cross-linked Pluronic nanocapsules. Presumably, the difference in the extent of volume transition is a result of the difference in their intrinsic properties of the three cross-linkers. Chitosan and heparin are soluble only in water, while PEI could be dissolved in both the organic and water phases. The capability of PEI to diffuse into the organic phase would lead to the formation of the thickest and tightest cross-linked wall.[31] In addition, chitosan has less charge when compared with PEI of similar molecular weight but has more charge than heparin. The electrostatic interaction between the cross-linkers in the nanocapsule wall could resist contraction during heating, which could explain why at 37 °C the Pluronic F127−PEI nanocapsules (∼90 nm) are much bigger than the Pluronic F127−chitsoan nanocapsules (∼37 nm) and the Pluronic F127−heparin nanocapsules (∼32 nm). Taken together, the thermal responsiveness in size (and the empty core−shell rather than a solid micelle structure) of the Pluronic F127-based nanocapsules presumably is a result of the complicated balance between the temperature-dependent hydrophobic interactions (leading to temperature-dependent volume contraction and expansion) within the Pluronic F127, the cross-link interaction between Pluronic F127 and chitosan to resist overexpansion at low temperatures, and electrostatic interaction between the cross-linker molecules to resist collapse at high temperatures.

In view of the more than 200 times change in volume of the Pluronic F127−chitosan nanocapsules in aqueous solution between 4 and 37 °C, one might hypothesize that the wall-permeability of the nanocapsules should be thermally responsive, as well: it should be high at 4 °C when the nanocapsules are swollen and low at 37 °C when the nanocapsules are shrunken. We validated this hypothesis by encapsulating a small fluorescence probe (ethidium bromide or EB) in the nanocapsules for temperature-controlled release and intracellular delivery, as demonstrated in Figures 6 and 7.

It has been shown that both hydrophilic and hydrophobic therapeutic agents with a molecular weight greater than 1 kD can be effectively withheld in appropriately designed Pluronic-based hydrogel or nanocapsules with minimum release for up to 2 days at a temperature above their LCST.[29,36] The results from this study demonstrate that the Pluronic F127-based nanocapsules are capable of withholding even smaller molecular weight molecules (*i.e.*, EB, MW = 394.3 Da) at 37 °C. Moreover, by utilizing their temperature-dependent wall-permeability, the nanocapsules were used to successfully encapsulate small molecules post their synthesis in this study, while in the literature, therapeutic agents (including anticancer drugs) were directly encapsulated in the hydrogel or nanocapsules during their synthesis.[29,36] This new approach allows the processes of nanocapsule synthesis and drug encapsulation to be performed at different times, which can significantly reduce the shipping and maintenance cost. In addition, the nanocapsule wall-permeability can be controlled by altering the time of EDC catalysis, Pluronic concentration, and presumably chitosan concentration according to Figures 3−6. Therefore, we believe this novel approach for encapsulation utilizing the temperature-dependent wall-permeability of the Pluronic-based nanocapsules is of great importance to encapsulate therapeutic agents of various molecular weights for intracellular delivery and temperature-controlled release.

The results shown in Figure 8 demonstrate the importance of thermal responsiveness in size of the nanocapsules for cellular uptake.[31,32] For example, the small size (∼37 nm) of the nanocapsules at 37 °C is important for cellular uptake because the nanocapsules must be small enough to be enwrapped in the endosome (∼150 nm) before they can be internalized by the cells *via* endocytosis. After internalization, the nanocapsules can mechanically break and escape the endosome/lysosome system as a result of the more than 200 times volume expansion in response to a cold shock treatment at 4 °C. Moreover, water sucked into the nanocapsules during the cooling phase can dissolve the encapsulated small molecules so that they can be released into the cytosol when the cells are heated back to 37 °C, as dem-

onstrated in Figures 6 and 7 using EB. Of note, the capability of the nanocapsules to break the endosome/lysosome and release the encapsulated small molecules into the cytosol in response to a cold shock treatment is of critical importance for intracellular delivery of the molecules. This is because drug degradation (for biodegradable nanoparticles encapsulated with pH and enzyme sensitive molecules) in the strongly acidic and enzymatic endosome/lysosome and exocytosis (for slowly or nonbiodegradable nanoparticles) of the encapsulated molecules has been reported to be a major bottleneck for cytosolic drug delivery using nanoparticles.[3,63−65]

Figures 7 and 8 also demonstrate that a significant amount of nanocapsules could be internalized by the MCF-7 cells in a short incubation period of 45 min, indicating that an accelerated endocytosis (rather than pinocytosis) was involved in the uptake process.[63−65] The accelerated endocytosis (also called adsorptive endocytosis)[66] presumably is due to the positively charged surface of the nanocapsules (because of the cross-linked chitosan, a polycation), which has a high affinity with the negatively charged cell plasma membrane as a result of electrostatic attraction. In short, as a result of its positively charged surface and thermal responsiveness in size and wall-permeability, the Pluronic F127−chitosan nanocapsules can be used to encapsulate small molecules (therapeutic agents) for intracellular delivery and temperature-controlled release into the cell cytosol. Of note, we used serum-free medium for the uptake studies. The presence of serum could interfere with cellular uptake of the nanocapsules, which can be resolved by surface modification of the nanocapsules with stealth molecules such as polyethylene glycol (PEG).[67−69]

We further demonstrated the nontoxic nature of the Pluronic F127−chitosan nanocapsule in Figure 9 (>99% immediate viability and normal proliferation), which could be attributed to the excellent biocompatibility of its constituent polymers. Pluronic F127 has been approved by the FDA for use as food additives and pharmaceutical ingredients.[34−37] Moreover, anticancer drugs encapsulated in Pluronic (including F127) micelles (not thermally responsive) have entered the stage of phase II clinical trial.[70−75] Chitosan is a natural polysaccharide that is commonly found in seafood and has been widely used for gene/drug delivery and tissue engineering due to its cationic and nontoxic nature.[42−47] A previous study showed that the immediate viability dropped to below ~95% when exposing mammalian cells to thermally responsive nanocapsules (1 mg/mL) made of Pluronic F127 and polyethylenimine (PEI) under the same experimental conditions,[33] which further indicates the superior biocompatibility of the Pluronic F127−chitosan nanocapsules reported here.

In summary, the nontoxic nature and the thermal responsiveness in size and wall-permeability make the Pluronic F127−chitosan nanocapsules unique to encapsulate small molecular weight therapeutic agents for the treatment of diseases (particularly cancer as a result of the differential uptake rate of the nanocapsules by cancerous *vs* noncancerous cells, as demonstrated in Figure 7). Moreover, the special property of the Pluronic F127−chitosan nanocapsules to release the encapsulated agents in response to a cold shock treatment makes them a natural combination of cryotherapy for destroying diseased tissue (using both drug and freezing) as the cooling and heating steps of cold shock are a natural part of a cryotherapy procedure that has been widely investigated as a minimally invasive alternative to radical surgical intervention in essentially all surgical subspecialties.[76−83] Lastly, the nanocapsules can be easily (because of the residual primary amine groups of chitosan on the nanocapsule surface) modified with stealth and targeting moieties for target-specific delivery to further enhance its specificity of targeting diseased rather than normal cells and tissues and reduce the drug systemic toxicity, which is ongoing in our lab.

MATERIALS AND METHODS

Materials. Pluronic F127 (MW = 12.6 kD) was kindly provided by BASF Corp. (Wyandotte, MI). Chitosan oligosaccharide of pharmaceutical grade (MW = 2.5 kD, 95% deacetylation) was obtained from Shanghai Weikang Biological Products Co. Ltd. (Shanghai, China). Ethidium bromide (EB), LysoTracker Red DND-99, and the live/dead viability/cytotoxicity assay kit were purchased from Invitrogen (Carlsbad, CA). The WST-1 cell proliferation reagent was purchased from Roche Diagnostics (Mannheim, Germany). The 4-dimethylaminopyridine (DMAP), 1,4-dioxane, triethylamine (TEA), succinic anhydride, and fluorescein isothiocyanate (FITC) were purchased from Sigma (St. Louis, MO) and used as received.

Synthesis of Pluronic F127−Chitosan Nanocapsules. To synthesize the Pluronic F127−chitosan nanocapsules, the chemically inert Pluronic F127 was first activated. A total of 6.3 g of Pluronic F127 and 122.17 mg of DMAP were dissolved in 15 mL of 1,4-dioxane with 139 μL of TEA. After stirring for 30 min under N_2 atmosphere, 125 mg of succinic anhydride in 5 mL of 1,4-dioxane was added dropwise into the solution. The mixture was stirred under N_2 atmosphere for 24 h at room temperature. The organic solvent (1,4-dioxane) was then removed by rotary evaporation, and the residual sample was filtered and precipitated in ice-cold diethyl ether three times. Finally, the precipitate was dried under vacuum overnight to obtain the white powder of dicarboxylated (activated) Pluronic F127.[49,84] The activation efficiency was determined using acid−base titration,[85] for which a total of 640 mg of activated Pluronic F127 was dissolved in 10 mL of deionized (DI) water (0.005 M). Titrations of the polymer solution with 1 M NaOH solution were performed at room temperature. Phenol red was used as a visual pH indicator, and the pH value was determined quantitatively using a pH meter.

The thermally responsive Pluronic F127−chitosan nanocapsules were prepared using a modified emulsification/solvent evaporation method (Figure 1). Briefly, a total of 100 mg of activated (dicarboxylated) Pluronic F127 and 5 mg of 1-ethyl-3-[3-

dimethylaminopropyl]carbodiimide hydrochloride (EDC for catalysis) were dissolved in 1 mL of dichloromethane (CH_2Cl_2) for 15 min to produce a 10% Pluronic F127 solution. To make a 30% solution of Pluronic F127 in 1 mL of dichloromethane, 300 mg of activated Pluronic F127 and 15 mg of EDC were used. The Pluronic F127 solution was added dropwise into a 10 mL aqueous solution of chitosan (7.5 mg/mL) at pH 5. The small molecular weight chitosan was used because of its good solubility in water and capability of diffusing into the matrix of Pluronic F127 to form cross-links not only on the surface but also inside the outer shell of the Pluronic micelle (Figure 1). The oil-in-water mixture was emulsified for 4 min using a Branson 450 sonifier (Danbury, CT). The emulsion was further stirred gently for up to 20 h to allow cross-link formation between the activated Pluronic F127 and chitosan on the aqueous side of the oil−water interface. The organic solvent (dichloromethane) in the emulsion was then removed by rotary evaporation until the solution became clear. The sample was further dialyzed against DI water with a Spectra/Por (Spectrum Laboratories, Rancho Dominguez, CA) dialysis tube (MWCO = 50 kD) for 1 day to remove EDC and any residual, non-cross-linked polymers.[33]

Characterization of the Nanocapsule Surface Chemistry, Morphology, and Size. Both FTIR (Fourier transform infrared) and ^{1}H NMR (proton nuclear magnetic resonance) spectroscopy were used to characterize the surface chemistry of the synthesized nanocapsules. For all FTIR studies, the Pluronic F127(10%)−chitosan nanocapsules were dissolved/suspended in dichloromethane, applied on the FTIR sample holder, and dried in a fume hood to form a homogeneously thin layer of nanocapsules on the holder. FTIR spectra (in the transmission mode) of the nanocapsule sample were then recorded at room temperature with dichloromethane as the control using a Shimadzu FTIR-8400 spectrometer and further analyzed using Origin (OriginLab, Northampton, MA). For the ^{1}H NMR studies, deuterated water (D_2O) was used as the solvent and the chemical shifts were measured in parts per million using D_2O as the internal reference. The ^{1}H NMR spectra were obtained using a Mercury Varian 400 NMR (Varian Inc., Palo Alto, CA) at room temperature.

The morphology of the nanocapsules was studied using transmission electron microscopy (TEM). For TEM analysis, one drop (2 μL) of the aqueous nanocapsule solution (2 mg/mL) was dried on a copper TEM grid for 10 min. The dried nanocapsule specimen was then stained by adding a drop (~2 μL) of 2% (w/v) uranyl acetate solution followed by drying for 10 min. The sample was then examined using a Hitachi H-800 transmission electron microscope. All of the procedures were performed at room temperature.

The size of the nanocapsules in physiologic (1×) PBS (phosphate buffered saline) at a concentration of 1 mg/mL at various temperatures from 4 to 45 °C was assessed *via* hydrodynamic radius measurements using a Wyatt (Santa Barbara, CA) DynaPro MSX dynamic light scattering (DLS) instrument and software.

Cell Culture. The noncancerous mesenchymal stromal (C3H10T1/2) cells derived from mouse embryos (ATCC, Manassas, VA) were cultured in high glucose DMEM supplemented with 10% fetal bovine serum, 100 U/mL penicillin and 100 μg/mL streptomycin at 37 °C in a humidified, 5% CO_2 incubator. Human breast cancer MCF-7 cells (ATCC) were cultured in the same way, except that the medium was further supplemented with 0.01 mg/mL insulin.

Encapsulation of Ethidium Bromide (EB) for Controlled Release and Intracellular Delivery. To encapsulate ethidium bromide (EB, a red fluorescence probe with a molecular weight of 394.3 Da that is usually excluded by healthy live cells[86,87]) in the Pluronic F127−chitosan nanocapsules, we first soaked the probe (3 mg) and nanocapsules (10 mg) in 300 μL of DI water overnight (~12 h) at 4 °C when the nanocapsules were swollen and their wall-permeability was high. The sample was then freeze-dried to remove water both inside and outside the nanocapsules. To obtain clean encapsulated EB without any free (non-encapsulated) EB outside the nanocapsules, the freeze-dried mixture of free and encapsulated EB was heated at 55 °C to shrink the nanocapsules, dissolved in 1 mL of DI water at 37 °C in a Spectra/Por CE Float-A-Lyzer G2 dialysis tube (MWCO = 50 kD), and dialyzed against 1 L of DI water at 37 °C for 10 h with the dialysis water being changed every ~3 h. The sample was then either used immediately or freeze-dried for future use.

For controlled release study, the clean encapsulated EB in 1 mL of DI water was further dialyzed against 45 mL of DI water at 37 °C with constant stirring in a beaker. After 3 h, a cold shock treatment was performed on the sample by transferring the sample into a centrifuge tube to cool for 15 min at 4 °C (in ice water). The sample was then transferred back to the dialysis tube and dialyzed against the 45 mL of water for another 3.5 h at 37 °C with constant stirring. A total of 0.5 mL of the 45 mL dialysate outside the dialysis tube in the beaker was collected at various times to determine the EB concentration in the dialysate colorimetrically using a UV/vis spectrometer (Beckman Coulter/DU 730), for which the absorbance of EB at 480 nm was measured and compared with a standard curve of the absorbance and EB concentration.[54,55] The standard curve was constructed by measuring the absorbance of EB in aqueous solutions of various known concentrations. The total volume of the dialysate outside the dialysis tube was kept at 45 mL by replenishing it with 0.5 mL of DI water at each sampling time.

To study intracellular delivery of EB for temperature-controlled release using the Pluronic F127(30%)−chitosan nanocapsules, MCF-7 and C3H10T1/2 cells were seeded in 33 mm Petri dishes at a density of 5×10^5 cells/dish in 1 mL medium. After 24 h, the culture medium was replaced with serum-free medium (1 mL) containing either 50 μL of the 1 mL clean encapsulated EB in the dialysis tube (which resulted in 0.5 mg/mL nanocapsules in the medium) or 50 μL of the last 1 L dialysis water used to remove non-encapsulated EB (without any EB-loaded nanocapsule in the medium for control). After incubating for 45 min at 37 °C, the cells were washed three times using warm (37 °C) 1× PBS. The cells were then fixed using 4% warm paraformaldehyde for 20 min at 37 °C either immediately or after a cold shock treatment to liberate the fluorescence probe from the nanocapsules by incubating the cells in 4 °C and then 37 °C 1× PBS for 15 min at each temperature. After fixation and washing twice using 1× PBS, the cell nuclei were stained with Hoechst 33342 (5 μM in 1× PBS for 10 min at room temperature) and further washed twice using 1× PBS. Intracellular distribution of EB in the cells was examined using a confocal microscope (LSM 510, Carl-Zeiss Inc., Oberkochen, Germany) by taking both DIC (differential interference contrast) and fluorescence (red and blue channels) images for further analysis.

Cellular Uptake of Pluronic F127−Chitosan Nanocapsules Labeled with Fluorescence Probe. To further our understanding of the mechanism by which mammalian cells take up the Pluronic F127−chitosan nanocapsules, we first labeled the nanocapsules with FITC, a green fluorescence probe. For the labeling, a total of 30 mg of the freeze-dried nanocapsules (synthesized using 10% Pluronic F127) was dissolved in 4.6 mL of 0.1 M sodium carbonate buffer at pH 9, followed by adding 110 μL of 26 mM FITC (in DMSO) into the solution in a dropwise manner. Permanent labeling of the nanocapsules with FITC was done by keeping the solution at 4 °C for 8 h with gentle and continuous shaking in the dark. A total of 6.1 mg of ammonium chloride was then added into the solution for 2 h at 4 °C to quench the labeling reaction. The FITC-labeled nanocapsules were purified (to remove DMSO, free FITC, and any other residual chemicals) by dialysis against DI water in the dark for 24 h with the water being changed every 3−5 h.

To study cellular uptake of the FITC-labeled nanocapsules, MCF-7 cells were seeded in 33 mm Petri dishes at a density of 5×10^5 cells/dish in 1 mL medium. After 24 h, the culture medium was replaced with serum-free medium containing FITC-labeled nanocapsules (0.5 mg/mL) and LysoTracker Red DND-99 (55 nM). The latter is a red fluorescence probe that can permeate cell plasma membrane and accumulates in subcellular organelles (the endosome/lysosome system) with an acidic environment. After incubation for 45 min at 37 °C, the cells were washed three times using warm (37 °C) 1× PBS. The cells were then fixed either immediately (for cells without a cold shock treatment at 4 °C) or after a cold shock treatment, nuclei stained with Hoechst 33342, and washed using 1× PBS for confocal microscopy study in the same way as that for the cells incubated with the EB-loaded nanocapsules. The time allowed for the cells either with

or without cold shock to take up the nanocapsules should be similar considering that 4 °C can shut down some endocytotic pathways.

Cytotoxicity of Pluronic F127—Chitosan Nanocapsules. Both immediate cell viability and long-term (3 day) cell proliferation were studied to test the cytotoxicity of the Pluronic F127−chitosan nanocapsules. For the immediate cell viability (*i.e.*, short-term toxicity) study, C3H10T1/2 and MCF-7 cells were seeded in 33 mm Petri dishes at a density of 2.5×10^5 and 5×10^5 cells/dish in 1 mL medium, respectively. After 24 h, the cell culture medium was replaced with warm (37 °C) serum-free medium containing Pluronic F127(30%)−chitosan nanocapsules of various concentrations up to 10 mg/mL. After incubating for 45 min at 37 °C, cells were washed three times using warm (37 °C) 1× PBS to remove any extracellular nanocapsules followed by a cold shock treatment in fresh culture medium for 15 min at 4 °C. Cell viability of the cells after cold shock followed by 15 min incubation at 37 °C was determined using the standard live/dead assay kit purchased from Invitrogen. The cells were examined using an Olympus BX 51 microscope equipped with fluorescent cubes and a QICAM CCD digital camera (QImaging, Surrey, BC, Canada). Immediate cell viability was calculated as the ratio of the number of viable cells to the total number (at least 1200 for each sample) of cells examined.

For long-term cell proliferation (long-term toxicity) studies, C3H10T1/2 and MCF-7 cells were seeded in 96-well plates at 1.25 and 2.5×10^4 cells/mL in 100 μL medium, respectively. At 24 h, the cells were exposed to the Pluronic F127(30%)−chitosan nanocapsules in the same way as that described above for immediate cell viability studies. After cold shock, the cells were further cultured for 3 days to monitor their proliferation. The Roche WST-1 assay was used to determine the cell numbers each day. Briefly, the medium was removed, and the cells were washed using 1× PBS. A total of 100 μL of fresh medium and 10 μL of the WST-1 assay were then added into each well. After incubating for 4 h, the absorbance at 440 nm of the sample in each well was determined using a Gen5 Synergy 2 plate reader (BioTek, Winooski, VT). Finally, the absorbance was converted to the number of cells using a standard curve of cell number *versus* the absorbance constructed by measuring the absorbance of samples with various known numbers of cells under the same experimental conditions.

Statistical Analysis. All results were reported as the mean ± standard deviation of data from at least three replicates. Student's two-tailed *t*-test assuming equal variance was calculated using Microsoft Excel to determine statistical significance ($p < 0.05$).

Acknowledgment. This work was supported by a grant (to X.H.) from the Wendy Will Case Cancer Fund and a University of South Carolina startup fund (to X.H.) from NSF (EPS-0447660).

REFERENCES AND NOTES

1. Breunig, M.; Bauer, S.; Goepferich, A. Polymers and Nanoparticles: Intelligent Tools for Intracellular Targeting. *Eur. J. Pharm. Biopharm.* **2008**, *68*, 112–128.
2. Tanaka, T.; Decuzzi, P.; Cristofanilli, M.; Sakamoto, J. H.; Tasciotti, E.; Robertson, F. M.; Ferrari, M. Nanotechnology for Breast Cancer Therapy. *Biomed. Microdevices* **2009**, *11*, 49–63.
3. Vasir, J. K.; Labhasetwar, V. Biodegradable Nanoparticles for Cytosolic Delivery of Therapeutics. *Adv. Drug Delivery Rev.* **2007**, *59*, 718–728.
4. Kumar, M. N. V. R. Nano and Microparticles as Controlled Drug Delivery Devices. *J. Pharm. Pharm. Sci.* **2000**, *3*, 234–258.
5. Vinogradov, S. V.; Bronich, T. K.; Kabanov, A. V. Nanosized Cationic Hydrogels for Drug Delivery: Preparation, Properties and Interactions with Cells. *Adv. Drug Delivery Rev.* **2002**, *54*, 135–147.
6. Stuart, M. A.; Huck, W. T.; Genzer, J.; Muller, M.; Ober, C.; Stamm, M.; Sukhorukov, G. B.; Szleifer, I.; Tsukruk, V. V.; Urban, M.; *et al.* Emerging Applications of Stimuli-Responsive Polymer Materials. *Nat. Mater.* **2010**, *9*, 101–113.
7. Caldorera-Moore, M.; Guimard, N.; Shi, L.; Roy, K. Designer Nanoparticles: Incorporating Size, Shape and Triggered Release into Nanoscale Drug Carriers. *Expert Opin. Drug Delivery* **2010**, *7*, 479–495.
8. Purushotham, S.; Chang, P. E.; Rumpel, H.; Kee, I. H.; Ng, R. T.; Chow, P. K.; Tan, C. K.; Ramanujan, R. V. Thermoresponsive Core−Shell Magnetic Nanoparticles for Combined Modalities of Cancer Therapy. *Nanotechnology* **2009**, *20*, 305101.
9. Tirelli, N. (Bio)Responsive Nanoparticles. *Curr. Opin. Colloid Interfaces* **2006**, *11*, 210–216.
10. Wei, H.; Zhang, X. Z.; Cheng, H.; Chen, W. Q.; Cheng, S. X.; Zhuo, R. X. Self-Assembled Thermo- and pH Responsive Micelles of Poly(10-undecenoic acid-B-*N*-isopropylacrylamide) for Drug Delivery. *J. Controlled Release* **2006**, *116*, 266–274.
11. Bolinger, P. Y.; Stamou, D.; Vogel, H. Integrated Nanoreactor Systems: Triggering the Release and Mixing of Compounds inside Single Vesicles. *J. Am. Chem. Soc.* **2004**, *126*, 8594–8595.
12. Palankar, R.; Skirtach, A. G.; Kreft, O.; Bedard, M.; Garstka, M.; Gould, K.; Mohwald, H.; Sukhorukov, G. B.; Winterhalter, M.; Springer, S. Controlled Intracellular Release of Peptides from Microcapsules Enhances Antigen Presentation on MHC Class I Molecules. *Small* **2009**, *5*, 2168–2176.
13. Injac, R.; Strukelj, B. Recent Advances in Protection against Doxorubicin-Induced Toxicity. *Technol. Cancer Res Treat.* **2008**, *7*, 497–516.
14. Ponce, A. M.; Vujaskovic, Z.; Yuan, F.; Needham, D.; Dewhirst, M. W. Hyperthermia Mediated Liposomal Drug Delivery. *Int. J. Hyperthermia* **2006**, *22*, 205–213.
15. Han, H. D.; Choi, M. S.; Hwang, T.; Song, C. K.; Seong, H.; Kim, T. W.; Choi, H. S.; Shin, B. C. Hyperthermia-Induced Antitumor Activity of Thermosensitive Polymer Modified Temperature-Sensitive Liposomes. *J. Pharm. Sci.* **2006**, *95*, 1909–1917.
16. Kong, G.; Dewhirst, M. W. Hyperthermia and Liposomes. *Int. J. Hyperthermia* **1999**, *15*, 345–370.
17. Unezaki, S.; Maruyama, K.; Takahashi, N.; Koyama, M.; Yuda, T.; Suginaka, A.; Iwatsuru, M. Enhanced Delivery and Antitumor Activity of Doxorubicin Using Long-Circulating Thermosensitive Liposomes Containing Amphipathic Polyethylene Glycol in Combination with Local Hyperthermia. *Pharm. Res.* **1994**, *11*, 1180–1185.
18. Iga, K.; Hamaguchi, N.; Igari, Y.; Ogawa, Y.; Gotoh, K.; Ootsu, K.; Toguchi, H.; Shimamoto, T. Enhanced Antitumor Activity in Mice after Administration of Thermosensitive Liposome Encapsulating Cisplatin with Hyperthermia. *J. Pharmacol. Exp. Ther.* **1991**, *257*, 1203–1207.
19. Purushotham, S.; Ramanujan, R. V. Thermoresponsive Magnetic Composite Nanomaterials for Multimodal Cancer Therapy. *Acta Biomater.* **2010**, *6*, 502–510.
20. Sershen, S. R.; Westcott, S. L.; Halas, N. J.; West, J. L. Temperature-Sensitive Polymer−Nanoshell Composites for Photothermally Modulated Drug Delivery. *J. Biomed. Mater. Res.* **2000**, *51*, 293–298.
21. Gao, C. Y.; Mohwald, H.; Shen, J. C. Thermosensitive Poly(allylamine)-G-Poly(*N*-isopropylacrylamide): Synthesis, Phase Separation and Particle Formation. *Polymer* **2005**, *46*, 4088–4097.
22. Gao, H. F.; Yang, W. L.; Min, K.; Zha, L. S.; Wang, C. C.; Fu, S. K. Thermosensitive Poly(*N*-isopropylacrylamide) Nanocapsules with Controlled Permeability. *Polymer* **2005**, *46*, 1087–1093.
23. Kang, S. I.; Na, K.; Bae, Y. H. Physicochemical Characteristics and Doxorubicin-Release Behaviors of pH/Temperature-Sensitive Polymeric Nanoparticles. *Colloid Surf. A* **2003**, *231*, 103–112.
24. Na, K.; Lee, K. H.; Lee, D. H.; Bae, Y. H. Biodegradable Thermo-Sensitive Nanoparticles from Poly(L-lactic acid)/Poly(ethylene glycol) Alternating Multi-Block Copolymer for Potential Anti-Cancer Drug Carrier. *Eur. J. Pharm. Sci.* **2006**, *27*, 115–122.
25. Ramkissoon-Ganorkar, C.; Gutowska, A.; Liu, F.; Baudys, M.;

Kim, S. W. Polymer Molecular Weight Alters Properties of pH-/Temperature-Sensitive Polymeric Beads. *Pharm. Res.* **1999**, *16*, 819–827.
26. Shen, Z.; Wei, W.; Zhao, Y.; Ma, G.; Dobashi, T.; Maki, Y.; Su, Z.; Wan, J. Thermosensitive Polymer-Conjugated Albumin Nanospheres as Thermal Targeting Anti-Cancer Drug Carrier. *Eur. J. Pharm. Sci.* **2008**, *35*, 271–282.
27. Liu, X. M.; Yang, Y. Y.; Leong, K. W. Thermally Responsive Polymeric Micellar Nanoparticles Self-Assembled from Cholesteryl End-Capped Random Poly(*N*-isopropylacrylamide-*co*-*N*,*N*-dimethylacrylamide): Synthesis, Temperature-Sensitivity, and Morphologies. *J. Colloid Interface Sci.* **2003**, *266*, 295–303.
28. Bae, K. H.; Choi, S. H.; Park, S. Y.; Lee, Y.; Park, T. G. Thermosensitive Pluronic Micelles Stabilized by Shell Cross-Linking with Gold Nanoparticles. *Langmuir* **2006**, *22*, 6380–6384.
29. Bae, K. H.; Lee, Y.; Park, T. G. Oil-Encapsulating PEO-PPO-PEO/PEG Shell Cross-Linked Nanocapsules for Target-Specific Delivery of Paclitaxel. *Biomacromolecules* **2007**, *8*, 650–656.
30. Choi, S. H.; Lee, J. H.; Choi, S. M.; Park, T. G. Thermally Reversible Pluronic/Heparin Nanocapsules Exhibiting 1000-Fold Volume Transition. *Langmuir* **2006**, *22*, 1758–1762.
31. Choi, S. H.; Lee, S. H.; Park, T. G. Temperature-Sensitive Pluronic/Poly(ethylenimine) Nanocapsules for Thermally Triggered Disruption of Intracellular Endosomal Compartment. *Biomacromolecules* **2006**, *7*, 1864–1870.
32. Lee, S. H.; Choi, S. H.; Kim, S. H.; Park, T. G. Thermally Sensitive Cationic Polymer Nanocapsules for Specific Cytosolic Delivery and Efficient Gene Silencing of SiRNA: Swelling Induced Physical Disruption of Endosome by Cold Shock. *J. Controlled Release* **2008**, *125*, 25–32.
33. Zhang, W.; Rong, J.; Wang, Q.; He, X. The Encapsulation and Intracellular Delivery of Trehalose Using a Thermally Responsive Nanocapsule. *Nanotechnology* **2009**, *20*, 275101.
34. Xiong, X. Y.; Tam, K. C.; Gan, L. H. Synthesis and Thermally Responsive Properties of Novel Pluronic F87/Polycaprolactone (PCL) Block Copolymers with Short PCL Blocks. *J. Appl. Polym. Sci.* **2006**, *100*, 4163–4172.
35. Wittemann, A.; Azzam, T.; Eisenberg, A. Biocompatible Polymer Vesicles from Biamphiphilic Triblock Copolymers and Their Interaction with Bovine Serum Albumin. *Langmuir* **2007**, *23*, 2224–2230.
36. Lee, S. H.; Lee, J. E.; Baek, W. Y.; Lim, J. O. Regional Delivery of Vancomycin Using Pluronic F-127 To Inhibit Methicillin Resistant *Staphylococcus aureus* (MRSA) Growth in Chronic Otitis Media *In Vitro* and *In Vivo*. *J. Controlled Release* **2004**, *96*, 1–7.
37. Alexandridis, P.; Hatton, T. A. Poly(ethylene oxide)-Poly(propylene oxide)-Poly(ethylene oxide) Block-Copolymer Surfactants in Aqueous-Solutions and at Interfaces—Thermodynamics, Structure, Dynamics, and Modeling. *Colloid Surf. A* **1995**, *96*, 1–46.
38. Fischer, D.; Li, Y.; Ahlemeyer, B.; Krieglstein, J.; Kissel, T. *In Vitro* Cytotoxicity Testing of Polycations: Influence of Polymer Structure on Cell Viability and Hemolysis. *Biomaterials* **2003**, *24*, 1121–1131.
39. Fischer, D.; Bieber, T.; Li, Y.; Elsasser, H. P.; Kissel, T. A Novel Non-Viral Vector for DNA Delivery Based on Low Molecular Weight, Branched Polyethylenimine: Effect of Molecular Weight on Transfection Efficiency and Cytotoxicity. *Pharm. Res.* **1999**, *16*, 1273–1279.
40. Tseng, W. C.; Jong, C. M. Improved Stability of Polycationic Vector by Dextran-Grafted Branched Polyethylenimine. *Biomacromolecules* **2003**, *4*, 1277–1284.
41. Moghimi, S. M.; Symonds, P.; Murray, J. C.; Hunter, A. C.; Debska, G.; Szewczyk, A. A Two-Stage Poly(ethylenimine)-Mediated Cytotoxicity: Implications for Gene Transfer/Therapy. *Mol. Ther.* **2005**, *11*, 990–995.
42. Lee, M.; Nah, J. W.; Kwon, Y.; Koh, J. J.; Ko, K. S.; Kim, S. W. Water-Soluble and Low Molecular Weight Chitosan-Based Plasmid DNA Delivery. *Pharm. Res.* **2001**, *18*, 427–431.
43. Jiang, X.; Dai, H.; Leong, K. W.; Goh, S. H.; Mao, H. Q.; Yang, Y. Y. Chitosan-G-PEG/DNA Complexes Deliver Gene to the Rat Liver *via* Intrabiliary and Intraportal Infusions. *J. Gene Med.* **2006**, *8*, 477–487.
44. Kim, T. H.; Nah, J. W.; Cho, M. H.; Park, T. G.; Cho, C. S. Receptor-Mediated Gene Delivery into Antigen Presenting Cells Using Mannosylated Chitosan/DNA Nanoparticles. *J. Nanosci. Nanotechnol.* **2006**, *6*, 2796–2803.
45. Dang, J. M.; Leong, K. W. Natural Polymers for Gene Delivery and Tissue Engineering. *Adv. Drug Delivery Rev.* **2006**, *58*, 487–499.
46. Prabaharan, M. Review Paper: Chitosan Derivatives as Promising Materials for Controlled Drug Delivery. *J. Biomater. Appl.* **2008**, *23*, 5–36.
47. Masotti, A.; Ortaggi, G. Chitosan Micro- and Nanospheres: Fabrication and Applications for Drug and DNA Delivery. *Mini-Rev. Med. Chem.* **2009**, *9*, 463–469.
48. Liu, T. Y.; Liu, K. H.; Liu, D. M.; Chen, S. Y.; Chen, I. W. Temperature-Sensitive Nanocapsules for Controlled Drug Release Caused by Magnetically Triggered Structural Disruption. *Adv. Funct. Mater.* **2009**, *19*, 616–623.
49. Park, K. M.; Bae, J. W.; Joung, Y. K.; Shin, J. W.; Park, K. D. Nanoaggregate of Thermosensitive Chitosan−Pluronic for Sustained Release of Hydrophobic Drug. *Colloid Surf. B* **2008**, *63*, 1–6.
50. Hoven, V. P.; Tangpasuthadol, V.; Angkitpaiboon, Y.; Vallapa, N.; Kiatkamjornwong, S. Surface-Charged Chitosan: Preparation and Protein Adsorption. *Carbohydr. Polym.* **2007**, *68*, 44–53.
51. Lawrie, G.; Keen, I.; Drew, B.; Chandler-Temple, A.; Rintoul, L.; Fredericks, P.; Grondahl, L. Interactions between Alginate and Chitosan Biopolymers Characterized Using FTIR and XPS. *Biomacromolecules* **2007**, *8*, 2533–2541.
52. K.C., R. B.; Lee, S. M.; Yoo, E. S.; Choi, J. H.; Ghim, H. D. Glycocojugated Chitosan Stabilized Iron Oxide Nanoparticles as a Multifuntional Nanoprobe. *Mater. Sci. Eng., C* **2009**, *29*, 1668–1673.
53. Heacock, R. A.; Marion, L. The Infrared Spectra of Secondary Amines and Their Salts. *Can. J. Chem.* **1956**, 34.
54. Dragan, A. I.; Bishop, E. S.; Strouse, R. J.; Casas-Finet, J. R.; Schenerman, M. A.; Geddes, C. D. Metal-Enhanced Ethidium Bromide Emission: Application to dsDNA Detection. *Chem. Phys. Lett.* **2009**, *480*, 296–299.
55. Pal, S. K.; Mandal, D.; Bhattacharyya, K. Photophysical Processes of Ethidium Bromide in Micelles and Reverse Micelles. *J. Phys. Chem. B* **1998**, *102*, 11017–11023.
56. Vardevanyan, P. O.; Antonyan, A. P.; Parsadanyan, M. A.; Davtyan, H. G.; Boyajyan, Z. R.; Karapetian, A. T. Complex-Formation of Ethidium Bromide with Poly[D(a-T)] · Poly[D(a-T)]. *J. Biomol. Struct. Dyn.* **2005**, *22*, 465–470.
57. Green, F. J. *The Sigma-Aldrich Handbook of Stains, Dyes and Indicators*; Aldrich Chemical Co., Inc.: Milwaukee, WI, 1990.
58. Severini, A.; Morgan, A. R. An Assay for Proteinases and Their Inhibitors Based on DNA/Ethidium Bromide Fluorescence. *Anal. Biochem.* **1991**, *193*, 83–89.
59. Scaria, P. V.; Shafer, R. H. Binding of Ethidium Bromide to a DNA Triple Helix. Evidence for Intercalation. *J. Biol. Chem.* **1991**, *266*, 5417–5423.
60. Griffiths, G.; Back, R.; Marsh, M. A Quantitative Analysis of the Endocytic Pathway in Baby Hamster Kidney Cells. *J. Cell Biol.* **1989**, *109*, 2703–2720.
61. Rejman, J.; Oberle, V.; Zuhorn, I. S.; Hoekstra, D. Size-Dependent Internalization of Particles *via* the Pathways of Clathrin- and Caveolae-Mediated Endocytosis. *Biochem. J.* **2004**, *377*, 159–169.
62. Kabanov, A. V.; Batrakova, E. V.; VY., A. Pluronic Block Copolymers as Novel Polymer Therapeutics for Drug and Gene Delivery. *J. Controlled Release* **2002**, *82*, 189–212.
63. Lloyd, J. B. Lysosome Membrane Permeability: Implications for Drug Delivery. *Adv. Drug Delivery Rev.* **2000**, *41*, 189–200.
64. Maxfield, F. R.; McGraw, T. E. Endocytic Recycling. *Nat. Rev. Mol. Cell Biol.* **2004**, *5*, 121–132.
65. McGraw, T. E.; Maxfield, F. R. *Targeted Drug Delivery*; Springer-Verlag: New York, 1991.

66. Callahan, J.; Kopecek, J. Semitelechelic HPMA Copolymers Functionalized with Triphenylphosphonium as Drug Carriers for Membrane Transduction and Mitochondrial Localization. *Biomacromolecules* **2006**, *7*, 2347–2356.
67. Joralemon, M. J.; McRae, S.; Emrick, T. Pegylated Polymers for Medicine: From Conjugation to Self-Assembled Systems. *Chem. Commun.* **2010**, *46*, 1377–1393.
68. Wattendorf, U.; Merkle, H. P. PEGylation as a Tool for the Biomedical Engineering of Surface Modified Microparticles. *J. Pharm. Sci.* **2008**, *97*, 4655–4669.
69. Pasut, G.; Veronese, F. M. PEG Conjugates in Clinical Development or Use as Anticancer Agents: An Overview. *Adv. Drug Delivery Rev.* **2009**, *61*, 1177–1188.
70. Valle, J. W.; Armstrong, A.; Newman, C.; Alakhov, V.; Pietrzynski, G.; Brewer, J.; Campbell, S.; Corrie, P.; Rowinsky, E. K.; Ranson, M. A Phase 2 Study of Sp1049c, Doxorubicin in P-Glycoprotein-Targeting Pluronics, in Patients with Advanced Adenocarcinoma of the Esophagus and Gastroesophageal Junction. *Invest. New Drugs* **2010**, ePub: Feb. 24, 2010.
71. Davis, M. E.; Chen, Z. G.; Shin, D. M. Nanoparticle Therapeutics: An Emerging Treatment Modality for Cancer. *Nat. Rev. Drug Discovery* **2008**, *7*, 771–782.
72. Armstrong, A.; Brewer, J.; Newman, C.; Alakhov, V.; Pietrzynski, G.; Campbell, S.; Corrie, P.; M., R.; Valle, J. W. Sp1049c as First-Line Therapy in Advanced (Inoperable or Metastatic) Adenocarcinoma of the Oesophagus: A Phase II Window Study. *J. Clin. Oncol.* **2006**, *24*, 4080.
73. Minko, T.; Batrakova, E. V.; Li, S.; Li, Y.; Pakunlu, R. I.; Alakhov, V. Y.; Kabanov, A. V. Pluronic Block Copolymers Alter Apoptotic Signal Transduction of Doxorubicin in Drug-Resistant Cancer Cells. *J. Controlled Release* **2005**, *105*, 269–278.
74. Danson, S.; Ferry, D.; Alakhov, V.; Margison, J.; Kerr, D.; Jowle, D.; Brampton, M.; Halbert, G.; Ranson, M. Phase I Dose Escalation and Pharmacokinetic Study of Pluronic Polymer-Bound Doxorubicin (Sp1049c) in Patients with Advanced Cancer. *Br. J. Cancer* **2004**, *90*, 2085–2091.
75. Alakhov, V.; Klinski, E.; Li, S. M.; Pietrzynski, G.; Venne, A.; Batrakova, E.; Bronitch, T.; Kabanov, A. Block Copolymer-Based Formulation of Doxorubicin. From Cell Screen to Clinical Trials. *Colloid Surf. B* **1999**, *16*, 113–134.
76. Gage, A. A.; Baust, J. G. Cryosurgery for Tumors. *J. Am. Coll. Surg.* **2007**, *205*, 342–356.
77. Gage, A. A.; Baust, J. G. Cryosurgery for Tumors—A Clinical Overview. *Technol. Cancer Res. Treat.* **2004**, *3*, 187–199.
78. Littrup, P. J.; Ahmed, A.; Aoun, H. D.; Noujaim, D. L.; Harb, T.; Nakat, S.; Abdallah, K.; Adam, B. A.; Venkatramanamoorthy, R.; Sakr, W.; *et al.* CT-Guided Percutaneous Cryotherapy of Renal Masses. *J. Vasc. Interv. Radiol.* **2007**, *18*, 383–392.
79. Hinshaw, J. L.; Littrup, P. J.; Durick, N.; Leung, W.; Lee, F. T., Jr.; Sampson, L.; Brace, C. L. Optimizing the Protocol for Pulmonary Cryoablation: A Comparison of a Dual- and Triple-Freeze Protocol. *Cardiovasc. Intervent. Radiol.* **2010**, ePub: May 1, 2010.
80. Wang, H.; Littrup, P. J.; Duan, Y.; Zhang, Y.; Feng, H.; Nie, Z. Thoracic Masses Treated with Percutaneous Cryotherapy: Initial Experience with More Than 200 Procedures. *Radiology* **2005**, *235*, 289–298.
81. Kaufman, C. S.; Rewcastle, J. C. Cryosurgery for Breast Cancer. *Technol. Cancer. Res. Treat.* **2004**, *3*, 165–175.
82. Sabel, M. S.; Kaufman, C. S.; Whitworth, P.; Chang, H.; Stocks, L. H.; Simmons, R.; Schultz, M. Cryoablation of Early-Stage Breast Cancer: Work-in-Progress Report of a Multi-Institutional Trial. *Ann. Surg. Oncol.* **2004**, *11*, 542–549.
83. Littrup, P. J.; Jallad, B.; Chandiwala-Mody, P.; D'Agostini, M.; Adam, B. A.; Bouwman, D. Cryotherapy for Breast Cancer: A Feasibility Study without Excision. *J. Vasc. Interv. Radiol.* **2009**, *20*, 1329–1341.
84. Park, K. M.; Lee, S. Y.; Joung, Y. K.; Na, J. S.; Lee, M. C.; Park, K. D. Thermosensitive Chitosan−Pluronic Hydrogel as an Injectable Cell Delivery Carrier for Cartilage Regeneration. *Acta Biomater.* **2009**, *5*, 1956–1965.
85. Tian, Y.; Bromberg, L.; Lin, S. N.; Hatton, T. A.; Tam, K. C. Complexation and Release of Doxorubicin from Its Complexes with Pluronic P85-B-Poly(acrylic acid) Block Copolymers. *J. Controlled Release* **2007**, *121*, 137–145.
86. Vivero-Escoto, J. L.; Slowing, I. I.; Lin, V. S. Tuning the Cellular Uptake and Cytotoxicity Properties of Oligonucleotide Intercalator-Functionalized Mesoporous Silica Nanoparticles with Human Cervical Cancer Cells HeLa. *Biomaterials* **2010**, *31*, 1325–1333.
87. Sailer, B. L.; Nastasi, A. J.; Valdez, J. G.; Steinkamp, J. A.; Crissman, H. A. Interactions of Intercalating Fluorochromes with DNA Analyzed by Conventional and Fluorescence Lifetime Flow Cytometry Utilizing Deuterium Oxide. *Cytometry* **1996**, *25*, 164–172.